THE JOURNAL OF PHYSICAL CHEMISTRY Letters

Letter

pubs.acs.org/JPCL

Dynamics of Lithium Dendrite Growth and Inhibition: Pulse Charging Experiments and Monte Carlo Calculations

Asghar Aryanfar,[†] Daniel Brooks,[‡] Boris V. Merinov,[‡] William A. Goddard, III,[‡] Agustín J. Colussi,*[,†] and Michael R. Hoffmann*[,†]

[†]Linde Center for Global Environmental Science, [‡]Materials and Process Simulation Center, California Institute of Technology, Pasadena, California 91125, United States

Supporting Information

ABSTRACT: Short-circuiting via dendrites compromises the reliability of Li-metal batteries. Dendrites ensue from instabilities inherent to electrodeposition that should be amenable to dynamic control. Here, we report that by charging a scaled coin-cell prototype with 1 ms pulses followed by 3 ms rest periods the average dendrite length is shortened ∼2.5 times relative to those grown under continuous charging. Monte Carlo simulations dealing with Li^+ diffusion and electromigration reveal that experiments involving 20 ms pulses were ineffective because Li^+ migration in the strong electric fields converging to dendrite tips generates extended depleted layers that cannot be replenished by diffusion during rest periods. Because the application of pulses much shorter than the characteristic time $\tau_c \sim O(\sim 1\ ms)$ for polarizing electric double layers in our system would approach DC charging, we suggest that dendrite propagation can be inhibited (albeit not suppressed) by pulse charging within appropriate frequency ranges.

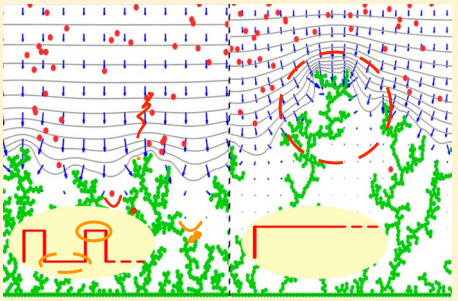

SECTION: Energy Conversion and Storage; Energy and Charge Transport

The specific high energy and power capacities of lithium metal (Li^0) batteries are ideally suited to portable devices and are valuable as storage units for intermittent renewable energy sources.[1−7] Li^0, the lightest and most electropositive metal, would be the optimal anode material for rechargeable batteries if it were not for the fact that such devices fail unexpectedly by short-circuiting via the dendrites that grow across electrodes upon recharging.[8,9] This phenomenon poses a major safety issue because it triggers a series of adverse events that start with overheating, which is potentially followed by the thermal decomposition and ultimately the ignition of the organic solvents used in such devices.[10−12]

Li^0 dendrites have been imaged, probed, and monitored with a wide array of techniques.[4,5,13] Moreover, their formation has been analyzed[14,15] and simulated at various levels of realism.[9,16,17] Numerous empirical and semiempirical strategies have been employed for mitigating the formation of Li^0 dendrites that were mostly based on modifications of electrode materials and morphologies and variations of operational conditions.[2] Thus, reports can be found on the effects of current density,[18−20] electrode surface morphology,[10] solvent and electrolyte composition,[21−24] electrolyte concentration,[18] evolution time,[25] the use of powder electrodes,[26] and adhesive lamellar block copolymer barriers[27] on dendrite growth. We suggest that further progress in this field should accrue from the deeper insights into the mechanism of dendrite propagation that could be gained by increasingly realistic and properly designed experiments and modeling calculations.[23,28] We considered that Li^0 dendrite nucleation and propagation are intrinsic to electrodeposition as a dynamic process under nonequilibrium conditions.[5,14] Furthermore, in contrast with purely diffusive crystal growth, that Li-ion (Li^+) electromigration is an essential feature of electrolytic dendrite growth.[29] More specifically, we envisioned that runaway dendrite propagation could be arrested by the relaxation of the steep Li^+ concentration gradients that develop around dendrite tips during charging. This is not a new strategy,[30] but to our knowledge the quantitative *statistical* impact of pulses of variable duration on dendrite length has not been reported before. Herein, we report experiments focusing on dendrite growth in a scaled coin cell prototype fitted with Li^0 electrodes charged with rectangular cathodic pulses of variable frequencies in the kilohertz range. We preserve the geometry and aspect ratio of commercial coin cells in our prototype, whose dimensions facilitate the visual observation of dendrites. The effects of pulsing on stochastic phenomena such as dendrite nucleation and growth are quantified for the first time on the basis of statistical averages of observed dendrite length distributions. We also present novel coarse-grained Monte Carlo model calculations that, by dealing explicitly with Li^+ migration in time-dependent nonuniform electric fields, provide valuable insights into the underlying phenomena. We believe our findings could motivate the design of safer charging

Received: January 29, 2014
Accepted: April 30, 2014
Published: April 30, 2014

Downloaded via CALIFORNIA INST OF TECHNOLOGY on April 5, 2021 at 20:27:07 (UTC).
See https://pubs.acs.org/sharingguidelines for options on how to legitimately share published articles.

 © 2014 American Chemical Society

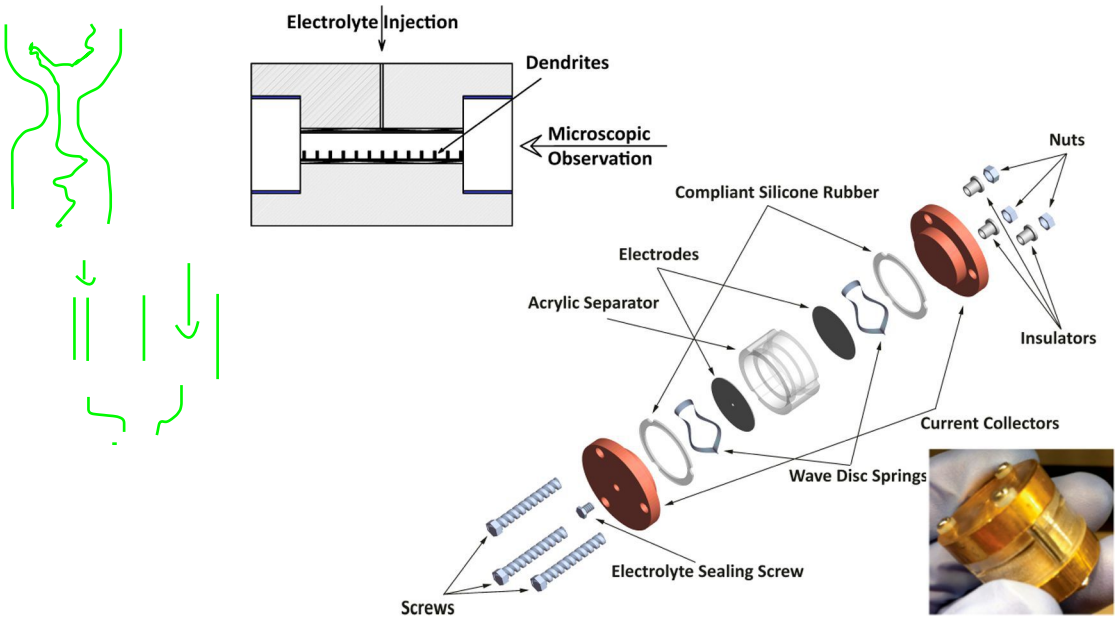

Figure 1. Top to bottom: cross section, exploded view, and physical appearance of the cell.

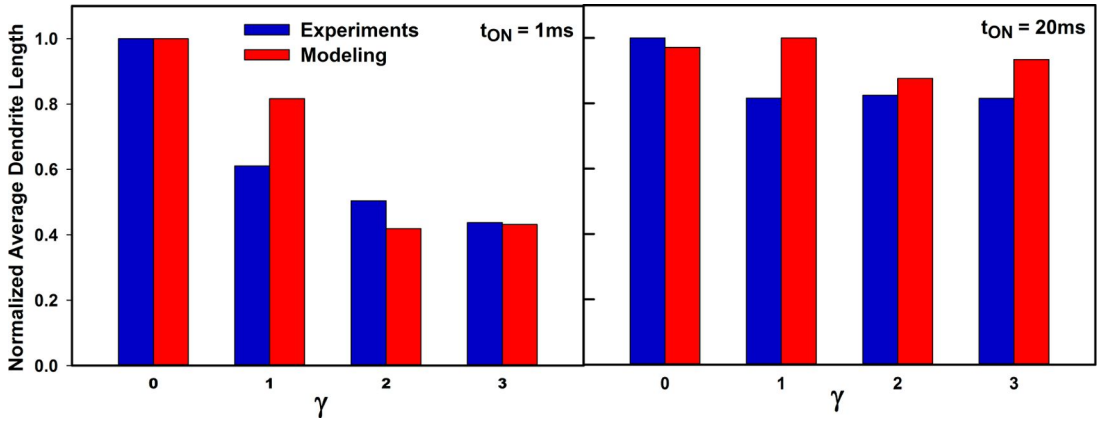

Figure 2. Pulse charging effects on average dendrite length α over a population of 45 dendrites grown on the perimeter of the Li^0 cathode. $\gamma = t_{OFF}/t_{ON}$ is the idle ratio.

protocols for commercial batteries. Current efforts in our laboratory aim at such goal.

We performed our experiments in a manually fabricated electrolytic cell that provides for in situ observation of the dendrites grown on the perimeter of the electrodes at any stage (Figure 1). The cell consists of two Li^0 foil disc electrodes (1.59 cm diameter) separated 0.32 cm by a transparent acrylic ring. The cell was filled with 0.4 cm^3 of 1 M $LiClO_4$ in propylene carbonate (PC) as electrolyte. We conducted all operations in an argon-filled (H_2O, O_2 < 0.5 ppm) glovebox. Arrays of multiple such cells were simultaneously electrolyzed with trains of 2 mA cm^{-2} pulses of variable t_{ON} durations and $\gamma = t_{OFF}/t_{ON}$ idle ratios generated by a programmable multichannel charger. After the passage of 48 mAh (173 Coulombs) through the cells, we measured the lengths of 45 equidistant dendrites grown on the cells perimeters by means of Leica M205FA optical microscope through the acrylic separator. Because dendrites propagate unimpeded in our device—that is, in the absence of a porous separator—our experiments are conducted under conditions for controlling dendrite propagation that are more adverse than those in actual commercial cells. Further details can be found in Experimental Details in the Supporting Information.

The lengths and multiplicities $[\lambda_i, p_i]$ of the 45 dendrites measured in series of experiments performed at t_{ON} = 1 and 20 ms, γ = 0 (DC), 1, 2, and 3, are shown as histograms in Figure S1 (Supporting Information). Dendrite lengths typically spanned the 200 μm−3000 μm range. Their average length α defined by eq 1

$$\alpha = \frac{\int p_i \lambda_i}{\int p_i} \tag{1}$$

represents a figure of merit more appropriate than the length of a single dendrite chosen arbitrarily for appraising the effect of pulsing on the outcome of stochastic processes. The resulting α values, normalized to the largest α in each set of experiments, are shown as blue bars as functions of γ for t_{ON} = 1 and 20 ms pulses in Figure 2. It is immediately apparent that the application of [t_{ON} = 1 ms; t_{OFF} = 3 ms] pulse trains reduces average dendrite lengths by ~2.4 times relative to DC charging, whereas t_{ON} = 20 ms pulses are rather ineffective at any γ.

dx.doi.org/10.1021/jz500207a | J. Phys. Chem. Lett. 2014, 5, 1721−1726

Basic arguments help clarify the physical meaning of the t_{ON} ~ 1 ms time scale. The mean diffusive (MSD) displacement of Li^+ ions, MSD = $(2\ D_+\ t)^{1/2}$ (where D_+ is the experimental diffusion coefficient of Li^+ in PC), defines the average thickness of the depletion layers created (via Faradaic reduction of Li^+ at the cathode) that could be replenished by diffusion during t rest periods.[15] Notice that MSD is a function of time$^{1/2}$ and depends on a property of the system (D_+), that is, it is independent of operating conditions such as current density. From the Einstein relationship, $D_+ = \mu_+ (RT/F)$[31] (μ_+ = is the mobility of Li^+ in PC), the electric fields $|E|_c$ at which Li^+ electromigration displacements, EMD = $\mu_+ |E|_c\ t$, that would match MSD are given by eq 2

$$|E|_c = (2RT/F)^{1/2} \mu_+^{-1/2} t^{-1/2} \tag{2}$$

Thus, with $(2\ RT/F)$ = 50 mV at 300 K, $\mu_+ = 1 \times 10^{-4}$ cm^2 V^{-1} s^{-1}, and t = 1 ms, we obtain $|E|_c$ = 707 V cm^{-1}, which is considerably stronger than the initial field between the flat parallel electrodes: $|E|_0 \sim V_0/L$ = 9.4 V cm^{-1}. Cathode flatness and field homogeneity, however, are destroyed upon the inception of dendrites, whose sharp (i.e., large radii of curvature) tips induce strong local fields.[15,32] Under such conditions, Li^+ will preferentially migrate to the tips of advancing dendrites rather than to flat or concave sectors of the cathode surface.[14,15,33−35] Because the stochastic nature of dendrite propagation necessarily generates a distribution of tip curvatures, the mean field condition EMD ≤ MSD at specified t_{ON} values is realized by a subset of the population of dendrites. On sharper dendrites the inequality EMD > MSD will apply at the end of t_{ON} pulses. Thus, larger $|E|_c$ values would extend the EMD ≤ MSD conditions to dendrites possessing sharper tips, that is, to a larger set of dendrites that could be controlled by pulsing. Note the weak $|E|_c \propto \mu_+^{-1/2} \propto \eta^{-1/2}$ dependence on solvent viscosity η.

From this perspective, because $|E|_c \propto t^{-1/2}$, the application of longer charging pulses will increase the width of the depletion layers over a larger subset of dendrites to such an extent that such layers could not be replenished during rest periods. The preceding analysis clearly suggests that shorter t_{ON} periods could be increasingly beneficial. Could t_{ON} be shortened indefinitely? No, because charging at sufficiently high frequencies will approach DC conditions. The transition from pulsed to DC charging will take place whenever t_{ON} becomes shorter than the characteristic times τ_c of the transients associated with the capacitive polarization of electrochemical double layers. This is so because under t_{ON} pulses shorter than τ_c most of the initial current will be capacitive, that is, polarization will significantly precede the onset of Faradaic interfacial electron transfer. A rule-of-thumb for estimating τ_c on "blocking" electrodes via eq 3[36−40]

$$\tau_c = \frac{\lambda_D L}{D_+} \tag{3}$$

leads to $\tau_c \sim 3.3$ ms. In eq 3, $\lambda_D = (\varepsilon(k_B T/2) z^2 e^2 C_0)^{1/2}$ is the Debye screening length, L the interelectrode gap, and D^+ the Li^+ diffusion coefficient. In our system, with C_0 = 1 M Li^+ solutions in PC (ε = 65), $D_+ = 2.58 \times 10^{-6}$ cm^2 s^{-1}, at 298 K, λ_D = 0.27. Because the double layer capacitance must be discharged via Faradaic currents in the ensuing rest periods,[41] it is apparent that the decreasing amplitude of polarization oscillations under trains of t_{ON} pulses much shorter than ~ τ_c will gradually converge to DC charging.

In summary, shorter t_{ON} pulses are beneficial for inhibiting dendrite propagation but are bound by the condition $t_{ON} \geq \tau_c$. The underlying reason is that shorter t_{ON} pulses inhibit dendrite at earlier propagation stages where the curvatures of most dendrite tips have not reached the magnitude at which local electric fields would lead to the EMD > MSD runaway condition. Notice that the stage at which dendrite propagation can be controlled by pulsing relates to the curvature of tip dendrites, which is a morphological condition independent of current density. Higher current densities, however, will shorten the induction periods preceding dendrite nucleation.[34]

These ideas were cast and tested in a coarse-grain Monte Carlo model that, in accord with the preceding arguments, deals explicitly with ion diffusion, electromigration, and deposition. It should be emphasized that our model is more realistic than those previously reported[9] because it takes into account the important fact that dendritic growth is critically dependent on the strong electric fields that develop about the dendrites tips upon charging.[42] The key role of electromigration in dendrite propagation has been dramatically demonstrated by the smooth Li^0 cathode surfaces produced in the presence of low concentrations of nonreducible cations, such as Cs^+ that, by preferentially accumulating on dendrite tips, neutralize local electric fields and deflect Li^+ toward the flat cathode regions.[3] Given the typically small overpotentials for metal ion reduction on metallic electrodes,[31] we consider that the effect of the applied external voltage on dendrite growth operates via the enhancement of Li^+ migration rather than accelerating Li^+ reduction. In other words, the population of electroactive Li^+ species within the partially depleted double layers surrounding the cathode should be established by the competition of ion diffusion versus electromigration rather than Li^+ deposition. Note furthermore that in our model dendrite nucleation is a purely statistical phenomenon, that is, nucleation occurs spontaneously because there is a finite probability that two or more Li^+ ions are successively reduced at a given spot on the cathode surface. Once a dendrite appears, a powerful positive feedback mechanism sets in. The enhanced electric field at the tip of the sharp dendrites draws in Li^+ ions faster, thereby accelerating dendrite growth/propagation and depleting the solution of Li^+ in its vicinity. The concentration gradients observed nearby growing dendrites are therefore deemed a consequence of the onset of dendrites. In our view, simultaneity does not imply causality,[43,44] that is, we consider that Li^+ depletion around dendrites is more of an effect rather than the cause of dendrite nucleation. Note, however, that experimentally indistinguishable mechanisms of dendrite *nucleation* are compatible with our interpretation that the effects of pulsing on dendrite *propagation* arise from the competition between ion diffusion and electromigration. Because of the computational cost of atomistic modeling, we simulate processes in a 2D domain that is smaller than the section of the actual cell. We chose its dimensions ($L^* \times L^*$ = 16.7 nm × 16.7 nm, Table 1) to exceed the depth of actual depletion boundary layers at the cathode. Because our calculations aim at reproducing the frequency response of our experiments, simulation time was set to real time. Therefore, to constrain within our domain the diffusional displacements occurring in real time, we used an appropriately scaled diffusion coefficient D_+^*. The adopted $D_+^* = 1.4 \times 10^{-10}$ cm^2/s = $5.6 \times 10^{-5}\ D_+$ value leads to MSD* ~ 0.3 L^* after 1 ms. The Einstein's relationship above ensures that this choice sets the scaled mobility at $\mu_+^* = D_+^* (F/RT) = 5.6 \times 10^{-9}$ cm^2/(V s).

dx.doi.org/10.1021/jz500207a | J. Phys. Chem. Lett. 2014, 5, 1721−1726

Table 1. Parameters Used in the Monte Carlo Calculations

domain size L	16.7 nm × 16.7 nm
Δt (integration step)	1 μs
$V_{cathode}$	0 V
V_{anode}	85 mV
D_+ (Li^+ diffusion coefficient)	1.4×10^{-10} cm^2/s
μ_+ (Li^+ mobility)	5.6×10^{-9} $cm^2/(V\ s)$
Li^+ radius	1.2 Å
free Li^+ ions	50
maximum Li^0 atoms	600

Then, in order to have EMD* $\cong \mu_+^* |E|^* t \sim$ MSD*, the scaled electric field mustbe $|E|^* = (V_{anode} - V_{cathode})^*/MSD^* = |E|_0/5.6 \times 10^{-5} = 1.7 \times 10^5$ V cm^{-1}, from which we obtain $(V_{anode} - V_{cathode})^* = MSD^* \cdot 1.7 \times 10^5$ V $cm^{-1} = 85$ mV. The two-dimensional Monte Carlo algorithm implemented on this basis calculates the trajectories of individual Li^+ ions via random diffusion and electromigration under time and position-dependent electric fields $\overrightarrow{E(x, y, t)}$.

By assuming that Li^+ ions reach stationary velocities instantaneously, their mean displacements are given by

$$\vec{r}_i(t + \Delta t) - \vec{r}_i(t) = \sqrt{2D_+\Delta t}\,\vec{g} + \mu_+\vec{E}\Delta t \quad (4)$$

The first and second terms in the RHS of eq 3 are the mean displacements due to ionic diffusion and electromigration, respectively. $\vec{g}$ is a normalized 2D vector representing random motion via diffusion, Δt is the computational time interval, and $\vec{E}$ is the electric field vector. By normalizing displacements relative to the interelectrode separation, L, eq 4 transforms into eq 5

$$\vec{\xi}(t + \Delta t) = \vec{\xi}(t) + \theta\vec{g} + \vec{\eta} \quad (5)$$

Dendrite lengths λ_i were evaluated as their height $\alpha_i(t)$ above the surface of the electrode

$$\lambda_i(t) = \max_{k=1:n} \vec{\xi}_k(t)\cdot\boldsymbol{j} \quad (6)$$

where $\boldsymbol{j}$ is the unit vector normal to the surface of the electrode and n is the total number of lithium atoms incorporated into the dendrite.

By using the Einstein relationship above, the equation of motion becomes

$$\vec{r}(t + \Delta t) - \vec{r}(t) = \sqrt{2D_+\Delta t}\,\hat{g} + \frac{F}{RT}D_+\Delta t\vec{E} \quad (7)$$

a function of $D_+\Delta t$.

By neglecting electrostatic ion−ion interactions, given that they are effectively screened because $\lambda_D = 0.27$ nm is smaller than the average interionic separation $R_{i,j} = 1.2$ nm, $\overrightarrow{E(x, y, t)}$ is computed using Laplace's equation

$$\frac{\partial^2\phi}{\partial x^2} + \frac{\partial^2\phi}{\partial y^2} = 0 \quad (8)$$

It is obvious that this approximation prevents our model to account for charge polarization, that is, the partial segregation of anions from cations under applied fields. Thus, in our calculations the electric field is instantaneously determined by the evolving geometry of the equipotential dendritic cathode. Note that the concentration gradients that develop in actual depleted boundary layers would lead to even greater electric field enhancements than reported herein. We were forced to adopt the approximation implicit in eq 8 because the inclusion of ion−ion interactions and charge imbalances would be forbiddingly onerous in calculations based on Monte Carlo algorithms. We consider, however, that the inclusion of a variable electric field represents a significant advance over previous models.[9]

Calculated dendrite heights were quantified by dividing the x axis (parallel to the surface of the cathode) in four sectors. Here, "dendrite height" in each sector is the height of the Li^0 atoms furthest from the electrode. To ensure good statistics, each simulation was run 100 times, for a total of 400 measurements per data point. The key experimental result, that is, that longer t_{OFF} rest periods are significantly more effective in reducing α after $t_{ON} = 1$ ms than $t_{ON} = 20$ ms charging pulses, is clearly confirmed by calculations (Figure 2 and Supporting Information Figure S1). Figure 3 displays the results of sample simulations. Metallic dendrites grow with random morphologies into equipotential structures held at $V =$ 0 V, thereby perturbing the uniform electric field prevailing at the beginning of the experiments. The high-curvature dendrite tips act as powerful attractors for the electric vector field, which by accelerating Li^+ toward their surfaces depletes the electrolyte self-enhances its intensity. This positive feedback mechanism has its counterpart in the electrolyte regions engulfed by dendrites because, by being surrounded with equipotential surfaces, Gauss's theorem ensures that the electric fields will nearly vanish therein.[31] It should be emphasized that the key feature is that ion displacements from electromigration are proportional to τ_{ON}, whereas diffusive ones increase as $\tau_{ON}^{1/2}$. Above some critical τ_{ON} value, the depth of the deplete layers will increase to the point at which they could not be replenished during the ensuing rest periods of any duration.

These phenomena are visualized from the computational results shown in Figures 3−6. Figure 4 displays the dendrite morphologies created by pulsing at various γ's. Calculations for longer t_{OFF} values show marginal improvements because $\partial[Li^+]/\partial y$ gradients remain largely unaffected in simulations for $\gamma > 3$. Figure 5 shows typical morphologies of dendrites consisting of a given number of deposited Li^0.

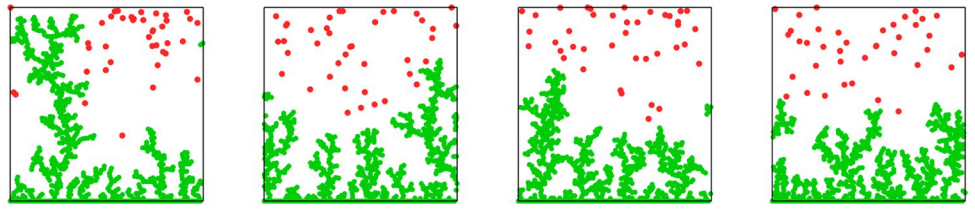

Figure 3. Left to right: dendrite morphologies for DC charging, charging with $t_{ON} = 1$ ms pulses at $\gamma = t_{OFF}/t_{ON} = 1$, 2, and 3. Green dots: Li^0. Red dots: Li^+.

dx.doi.org/10.1021/jz500207a | J. Phys. Chem. Lett. 2014, 5, 1721−1726

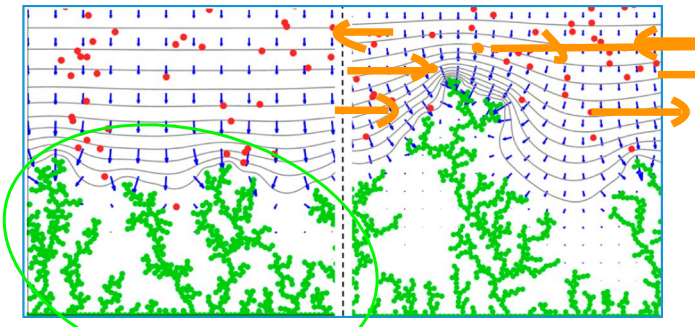

Figure 4. Simulations for charging with t_{ON} = 1 ms (left) and t_{ON} = 20 ms (right) at $\gamma = t_{OFF}/t_{ON} = 3$. Green dots: Li^0. Red dots: Li^+. Gray lines: equipotential contours. Blue vectors: the electric field.

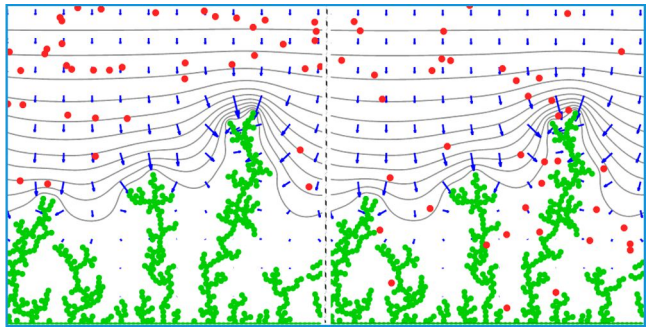

Figure 5. Simulations for charging with t_{ON} = 1 ms, γ = 1 pulses. Left: after a charging pulse. Right: at the end of the successive rest period (right). Green dots: Li^0. Red dots: Li^+. Gray lines: equipotential contours. Blue vectors: the electric field.

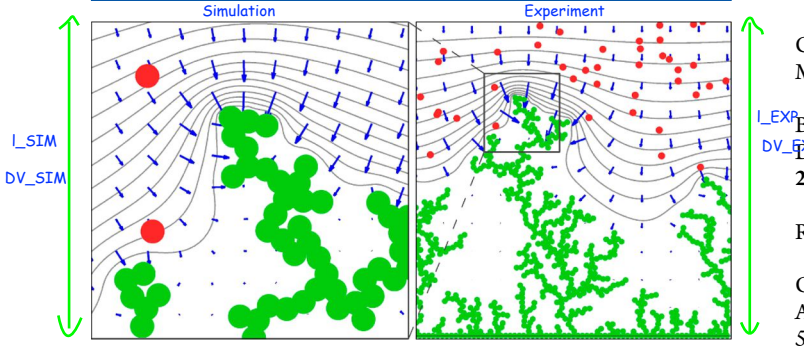

Figure 6. Zooming in the tip of the leading dendrite produced by charging with t_{ON} = 20 ms, $\gamma = t_{OFF}/t_{ON} = 3$ pulses for 243 ms, that is, at the end of simulation time. Green dots: Li^0. Red dots: Li^+. Gray lines: equipotential contours. Blue vectors: the electric field.

Summing up, we have demonstrated (1) that by charging our lithium metal cell with t_{ON} = 1 ms, $\gamma = t_{OFF}/t_{ON} = 3$ pulse trains, the average dendrite length α is significantly reduced (by ~70%) relative to DC charging and (2) that such pulses are nearly optimal for dendrite inhibition because they are commensurate with the relaxation time $\tau_c \sim 3$ ms for the diffusive charging of the electrochemical double layers in our system. Monte Carlo simulations dealing explicitly with lithium ion diffusion, electromigration in time-dependent electric fields, and deposition at the cathode are able to reproduce the experimental trends of t_{ON} on average dendrite lengths. Further work along these lines is underway.

■ ASSOCIATED CONTENT

Supporting Information

Additional data and experimental and calculational details are available free of charge via the Internet at http://pubs.acs.org/.

■ AUTHOR INFORMATION

Corresponding Authors

*A. J. C. E-mail: ajcoluss@caltech.edu.
*M. R. H. E-mail: mrh@caltech.edu.

Notes

The authors declare no competing financial interest.

■ ACKNOWLEDGMENTS

We thank undergraduate student Alejandro Sánchez for helping with the manufacture of cell parts. This work was sponsored by Bill and Melinda Gates Foundation Grant No. OPP1069500 on environmental sustainability and, in part, by Bosch Energy Research Network Grant No. 13.01.CC11.

■ REFERENCES

(1) Xu, W.; Wang, J.; Ding, F.; Chen, X.; Nasybulin, D.; Zhang, Y.; Zhang, J. G. Lithium Metal Anodes for Rechargeable Batteries. *Energy Environ. Sci.* **2014**, *7*, 513−537.
(2) Armand, M.; Tarascon, J. M. Building Better Batteries. *Nature* **2008**, *451*, 652−657.
(3) Ding, F.; Xu, W.; Graff, G. L.; Zhang, J.; Sushko, M.; Chen, X.; Shao, Y.; Engelhard, M. H.; Nie, Z.; Xiao, J. Dendrite-Free Lithium Deposition Via Self-Healing Electrostatic Shield Mechanism. *J. Am. Chem. Soc.* **2013**, *135*, 4450−4456.
(4) Chandrashekar, S.; Trease, N. M.; Chang, H. J.; Du, L.-S.; Grey, C. P.; Jerschow, A. ^{7}Li MRI of Li Batteries Reveals Location of Microstructural Lithium. *Nat. Mater.* **2012**, *11*, 311−315.
(5) Harry, K. J.; Hallinan, D. T.; Parkinson, D. Y.; MacDowell, A. A.; Balsara, N. P. Detection of Subsurface Structures Underneath Dendrites Formed on Cycled Lithium Metal Electrodes. *Nat. Mater.* **2014**, *13*, 69−73.
(6) Rugolo, J.; Aziz, M. J. Electricity Storage for Intermittent Renewable Sources. *Energy Environ. Sci.* **2012**, *5*, 7151−7160.
(7) Huskinson, B.; Marshak, M. P.; Suh, C.; Er, S.; Gerhardt, M. R.; Galvin, C. J.; Chen, X.; Aspuru-Guzik, A.; Gordon, R. G.; J. Aziz, M. J. A Metal-Free Organic−Inorganic Aqueous Flow Battery. *Nature* **2014**, *505*, 195−198.
(8) Goodenough, J. B. Rechargeable Batteries: Challenges Old and New. *J. Solid State Electrochem.* **2012**, *16*, 2019−2029.
(9) Mayers, M. Z.; Kaminski, J. W.; Miller, T. F., III Suppression of Dendrite Formation Via Pulse Charging in Rechargeable Lithium Metal Batteries. *J. Phys. Chem. C* **2012**, *116*, 26214−26221.
(10) Nishida, T.; Nishikawa, K.; Rosso, M.; Fukunaka, Y. Optical Observation of Li Dendrite Growth in Ionic Liquid. *Electrochim. Acta* **2013**, *100*, 333−341.
(11) Williard, N.; He, W.; Hendricks, C.; Pecht, M. Lessons Learned from the 787 Dreamliner Issue on Lithium-Ion Battery Reliability. *Energies* **2013**, *6*, 4682−4695.
(12) Xu, K. Nonaqueous Liquid Electrolytes for Lithium-Based Rechargeable Batteries. *Chem. Rev.* **2004**, *104*, 4303−4418.
(13) Nishikawa, K.; Mori, T.; Nishida, T.; Fukunaka, Y.; Rosso, M.; Homma, T. In Situ Observation of Dendrite Growth of Electrodeposited Li Metal. *J. Electrochem. Soc.* **2010**, *157*, A1212−A1217.
(14) Fleury, V. Branched Fractal Patterns in Non-Equilibrium Electrochemical Deposition from Oscillatory Nucleation and Growth. *Nature* **1997**, *390*, 145−148.
(15) Chazalviel, J. N. Electrochemical Aspects of the Generation of Ramified Metallic Electrodeposits. *Phys. Rev. A: At., Mol., Opt. Phys.* **1990**, *42*, 7355−7367.

(16) Ely, D. R.; Garcia, R. E. Heterogeneous Nucleation and Growth of Lithium Electrodeposits on Negative Electrodes. *J. Electrochem. Soc.* **2013**, *160*, A662−A668.
(17) Akolkar, R. Mathematical Model of the Dendritic Growth During Lithium Electrodeposition. *J. Power Sources* **2013**, *232*, 23−28.
(18) Brissot, C.; Rosso, M.; Chazalviel, J. N.; Lascaud, S. In Situ Concentration Cartography in the Neighborhood of Dendrites Growing in Lithium/Polymer-Electrolyte/Lithium Cells. *J. Electrochem. Soc.* **1999**, *146*, 4393−4400.
(19) Orsini, F.; D. P, A.; Beaudoin, B.; Tarascon, J. M.; Trentin, M.; Langenhuisen, N.; Beer, E. D.; Notten, P. In Situ Scanning Electron Microscopy (SEM) Observation of Interfaces with Plastic Lithium Batteries. *J. Power Sources* **1998**, *76*, 19−29.
(20) Monroe, C.; Newman, J. Dendrite Growth in Lithium/Polymer Systems—a Propagation Model for Liquid Electrolytes under Galvanostatic Conditions. *J. Electrochem. Soc.* **2003**, *150*, A1377−A1384.
(21) Crowther, O.; West, A. C. Effect of Electrolyte Composition on Lithium Dendrite Growth. *J. Electrochem. Soc.* **2008**, *155*, A806−A811.
(22) Howlett, P. C.; MacFarlane, D. R.; Hollenkamp, A. F. A Sealed Optical Cell for the Study of Lithium-Electrode Electrolyte Interfaces. *J. Power Sources* **2003**, *114*, 277−284.
(23) Schweikert, N.; Hofmann, A.; Schulz, M.; Scheuermann, M.; Boles, S. T.; Hanemann, T.; Hahn, H.; Indris, S. Suppressed Lithium Dendrite Growth in Lithium Batteries Using Ionic Liquid Electrolytes: Investigation by Electrochemical Impedance Spectroscopy, Scanning Electron Microscopy, and in Situ Li-7 Nuclear Magnetic Resonance Spectroscopy. *J. Power Sources* **2013**, *228*, 237−243.
(24) Basile, A.; Hollenkamp, A. F.; Bhatt, A. I.; O'Mullane, A. P. Extensive Charge−Discharge Cycling of Lithium Metal Electrodes Achieved Using Ionic Liquid Electrolytes. *Electrochem. Commun.* **2012**, *27*, 69−72.
(25) Rosso, M.; Gobron, T.; Brissot, C.; Chazalviel, J. N.; Lascaud, S. Onset of Dendritic Growth in Lithium/Polymer Cells. *J. Power Sources* **2001**, *97*−*8*, 804−806.
(26) Seong, I. W.; Hong, C. H.; Kim, B. K.; Yoon, W. Y. The Effects of Current Density and Amount of Discharge on Dendrite Formation in the Lithium Powder Anode Electrode. *J. Power Sources* **2008**, *178*, 769−773.
(27) Stone, G.; Mullin, S.; Teran, A.; Hallinan, D.; Minor, A.; Hexemer, A.; Balsara, N. Resolution of the Modulus Versus Adhesion Dilemma in Solid Polymer Electrolytes for Rechargeable Lithium Metal Batteries. *J. Electrochem. Soc.* **2012**, *159*, A222−A227.
(28) Bhattacharyya, R.; Key, B.; Chen, H. L.; Best, A. S.; Hollenkamp, A. F.; Grey, C. P. In Situ NMR Observation of the Formation of Metallic Lithium Microstructures in Lithium Batteries. *Nat. Mater.* **2010**, *9*, 504−510.
(29) Benjacob, E.; Garik, P. The Formation of Patterns in Nonequilibrium Growth. *Nature* **1990**, *343*, 523−530.
(30) Huggins, R. *Advanced Batteries: Material Science Aspects*; Springer: New York, 2008.
(31) Bard, A. J.; Faulkner, L. R. *Electrochemical Methods: Fundamentals and Applications*; Wiley: New York, 1980.
(32) Jackson, J. D. *Classical Electrodynamics*; Wiley: New York, 1999.
(33) Roy, S. Formation of Dual Diffusion Layer by Pulsing Currents. *Ind. Eng. Chem. Res.* **2012**, *51*, 1756−1760.
(34) Diggle, J.; Despic, A.; Bockris, J. M. The Mechanism of the Dendritic Electrocrystallization of Zinc. *J. Electrochem. Soc.* **1969**, *116*, 1503−1514.
(35) Wang, M.; Ming, N. B. Concentration Field Oscillation in Front of a Dendrite Tip in Electrochemical Deposition. *Phys. Rev. A: At., Mol., Opt. Phys.* **1992**, *45*, 2493−2498.
(36) Bazant, M. Z.; Thornton, K.; Ajdari, A. Diffuse-Charge Dynamics in Electrochemical Systems. *Phys. Rev. E: Stat., Nonlinear, Soft Matter Phys.* **2004**, *70*, No. 021506.
(37) Norton, J. D.; White, H. S.; Feldberg, S. W. Effect of the Electrical Double-Layer on Voltametry at Microelectrodes. *J. Phys. Chem.* **1990**, *94*, 6772−6780.
(38) Alexe-Ionescu, A. L.; Barbero, G.; Bianco, S.; Cicero, G.; Pirri, C. F. Electrical Response of Electrolytic Cells Limited by Different Types of Electrodes. *J. Electroanal. Chem.* **2012**, *669*, 21−27.
(39) Macdonald, J. R. Theory of AC Space-Charge Polarization Effects in Photoconductors, Semiconductors and Electrolytes. *Phys. Rev.* **1953**, *92*, 4−17.
(40) Hossain, R.; Adamiak, K. Dynamic Properties of the Electric Double Layer in Electrolytes. *J. Electrostat.* **2013**, *71*, 829−838.
(41) Ibl, N. Some Theoretical Aspects of Pulse Electrolysis. *Surface Technology* **1980**, *10*, 81−104.
(42) Zhong, X. K.; Guo, X. P.; Qiu, Y. B.; Chen, Z. Y.; Zhang, G. A. In Situ Study the Electrochemical Migration of Tin under Unipolar Square Wave Electric Field. *J. Electrochem. Soc.* **2013**, *160*, D495−D500.
(43) Leger, C.; Argoul, F.; Bazant, M. Z. Front Dynamics During Diffusion-Limited Corrosion of Ramified Electrodeposits. *J. Phys. Chem. B* **1999**, *103*, 5841−5851.
(44) Rosso, M. Electrodeposition from a Binary Electrolyte: New Developments and Applications. *Electrochim. Acta* **2007**, *53*, 250−256.

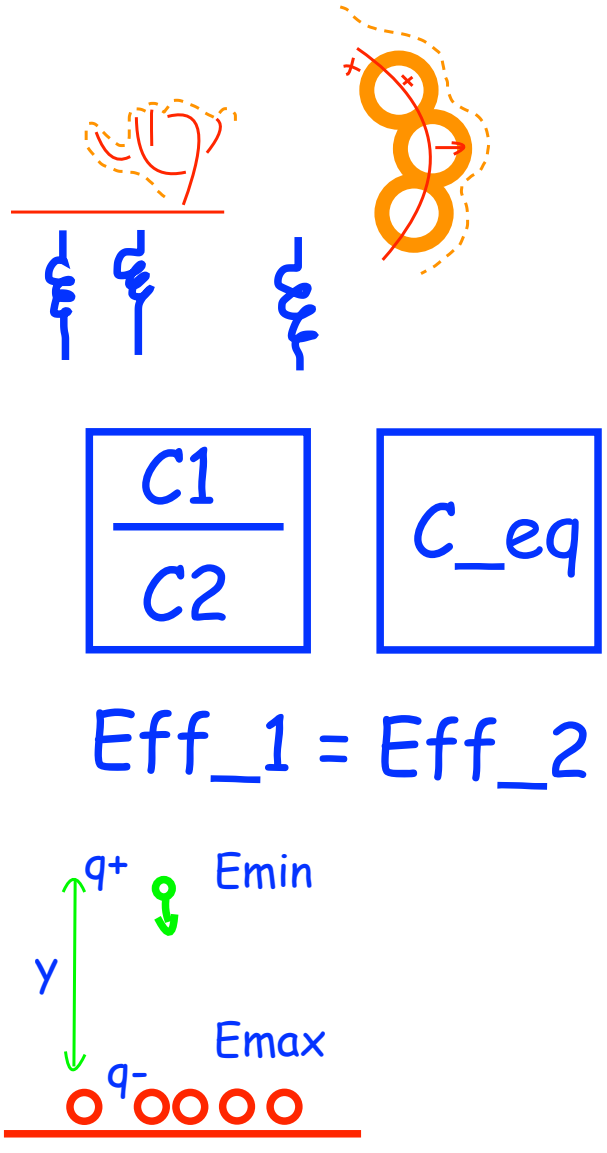

dx.doi.org/10.1021/jz500207a | *J. Phys. Chem. Lett.* 2014, 5, 1721−1726